

## Population Analysis of the Intermediate Complex States During B-Z Transition of Non-CG-repeat DNA Duplexes Induced by the Z $\alpha$ Domain of Human ADAR1

Eun-Hae Lee, Yeo-Jin Seo, Hee-Eun Kim, Yeon-Mi Lee, Chong-Man Kim,<sup>†,\*</sup> and Joon-Hwa Lee\*

Department of Chemistry and Research Institute of Natural Science, Gyeongsang National University, Gyeongnam 660-701, Korea. \*E-mail: joonhwa@gnu.ac.kr

<sup>†</sup>Department of Industrial and Management Engineering, Myongji University, Gyeonggi 449-728, Korea  
\*E-mail: chongman@mju.ac.kr

Received September 30, 2010, Accepted December 10, 2010

**Key Words:** NMR, Hydrogen exchange, Z-DNA, Confidence limit, ADAR1

Z-DNA contains nucleic acid bases in alternating *anti*- and *syn*-conformations along the nucleotide chain and has only one groove that is similar to the minor groove of B-DNA.<sup>1-3</sup> Z-DNA is in a higher energy conformation than B-DNA and is stabilized by negative supercoiling generated *in vivo*.<sup>2,3</sup> Human ADAR1 has two left-handed Z-DNA binding domains at its NH<sub>2</sub>-terminus, Z $\alpha$  and Z $\beta$ , preferentially binds Z-DNA, rather than B-DNA, with high binding affinity.<sup>4,6</sup> The co-crystal structure of the Z $\alpha$  domain of human ADAR1 (Z $\alpha$ <sub>ADAR1</sub>) bound to Z-DNA revealed that one monomeric Z $\alpha$ <sub>ADAR1</sub> domain binds to one strand of double-stranded DNA and a second Z $\alpha$ <sub>ADAR1</sub> monomer binds to the opposite strand with two-fold symmetry with respect to the DNA helical axis.<sup>7</sup> A structural study showed that Z $\alpha$ <sub>ADAR1</sub> binds to the Z-conformation of non-CG-repeat DNA duplexes through a common structural feature rather than by a specific sequence or structural alternations.<sup>8</sup> A previous NMR study on a d(CGCGCG)<sub>2</sub>-Z $\alpha$ <sub>ADAR1</sub> complex<sup>9</sup> suggests an *active-mono* B-Z transition mechanism (see Fig. 1) in which the Z $\alpha$ <sub>ADAR1</sub> protein first binds to B-DNA and then converts it to left-handed Z-DNA, a conformation that is then stabilized by the additional binding of a second Z $\alpha$ <sub>ADAR1</sub> molecule.

Recently, we have reported NMR hydrogen exchange data of complexes between Z $\alpha$ <sub>ADAR1</sub> and the non-CG-repeat DNA duplexes, d(CACGTG)<sub>2</sub> [referred to as CA6] or d(CGTACG)<sub>2</sub> [referred to as TA6], with a variety of protein-to-DNA (P/N) molar ratios.<sup>10</sup> The  $k_{ex}$  data for the G4b of the CA6-Z $\alpha$ <sub>ADAR1</sub> complex and for the G2b of the TA6-Z $\alpha$ <sub>ADAR1</sub> complex showed significant changes as the Z-DNA fraction ( $f_z$ ) was increased (meaning that the P/N ratio increased) (see Fig. 2). These changes of the  $k_{ex}$  data can be explained by the presence of mixtures of two imino protons from B-form DNA (referred to as **B**) and

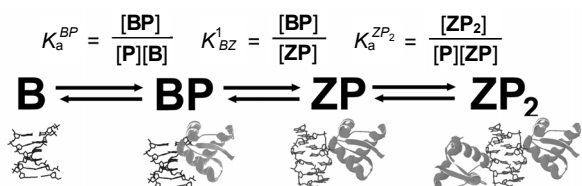


**Figure 1.** Active-mono B-Z transition mechanism of a 6-bp DNA duplex by two Z-DNA binding proteins. **B** and **Z** indicate the B-form and Z-form of the DNA duplex and **P** indicates the Z-DNA binding proteins.

B-DNA-Z $\alpha$ <sub>ADAR1</sub> complex (referred to as **BP**) in the imino peaks as given by Eq. 1:<sup>10</sup>

$$k_{ex} = \frac{[B]k_{ex}^B + [BP]k_{ex}^{BP}}{[B] + [BP]} = k_{ex}^B + \frac{[BP]}{1 - Z_t} (k_{ex}^{BP} - k_{ex}^B) \quad (1)$$

where  $k_{ex}^B$  and  $k_{ex}^{BP}$  are the  $k_{ex}$  of the imino protons for the **B** and

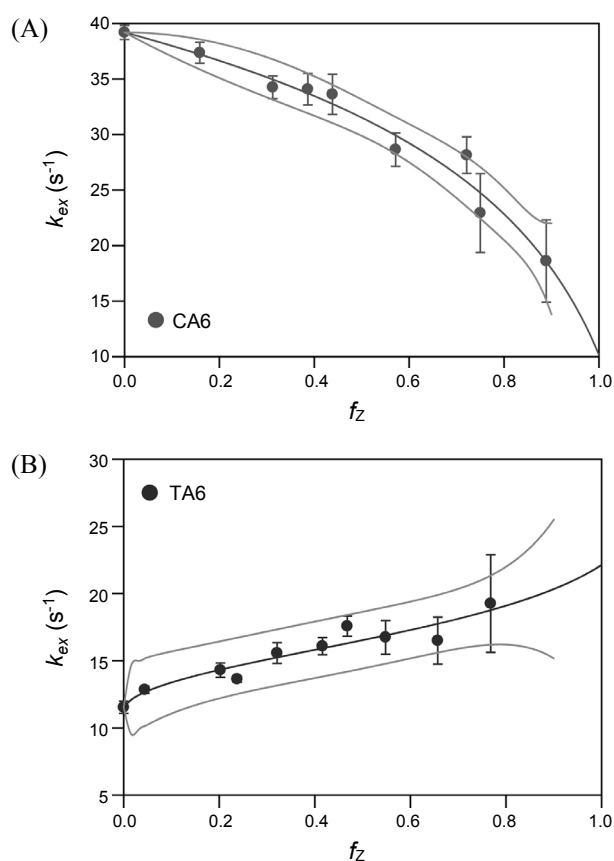


**Figure 2.** (A) The  $k_{ex}$  values of the G4b imino proton for the CA6-Z $\alpha$ <sub>ADAR1</sub> complex determined at 25 °C and (B)  $k_{ex}$  values of the G2b imino proton for the TA6-Z $\alpha$ <sub>ADAR1</sub> complex determined at 15 °C as a function of the  $f_z$ . Black solid lines are the best fit to Eq. 1, where the  $k_{ex}$  data were weighted by the inverse of their variance. The grey lines indicate their upper and lower confidence limits (95% confidence level).

**BP** states, respectively, and **[B]** and **[BP]** are the concentrations of the **B** and **BP** states,  $Z_t$  is the total concentration of Z-conformation. Thus, the correlation between the  $k_{ex}$  and  $f_Z$  data can be expressed by Eq. 2 as described in previous report:<sup>10</sup>

$$k_{ex} = k_{ex}^B + \frac{(k_{ex}^{BP} - k_{ex}^B)}{2(1-\alpha)(1-f_Z)} \left\{ 1 + (K_{BZ}^1 - 1)f_Z - \sqrt{(1 + (K_{BZ}^1 - 1)f_Z)^2 - 4K_{BZ}^1(1-\alpha)f_Z(1-f_Z)} \right\} \quad (2)$$

where  $K_{BZ}^1 = [\mathbf{BP}]/[\mathbf{ZP}]$ , and  $\alpha (= K_a^{ZP_2}/K_a^{BP})$  is the ratio of the association constants ( $K_a$ ) of the  $\mathbf{ZP}_2$  and  $\mathbf{BP}$  complex states. In the previous report,<sup>10</sup> the  $\alpha$  (CA6: 1.42; TA6: 13.9),  $K_{BZ}^1$  (CA6:  $0.4 \pm 0.1$ ; TA6:  $6.3 \pm 3.1$ ),  $k_{ex}^B$  (CA6:  $39.2 \pm 0.6 \text{ s}^{-1}$ ; TA6:  $11.5 \pm 0.5 \text{ s}^{-1}$ ), and  $k_{ex}^{BP}$  (CA6:  $10.2 \pm 3.1 \text{ s}^{-1}$ ; TA6:  $22.2 \pm 5.3 \text{ s}^{-1}$ ) values of CA6 and TA6 complexed with  $Z\alpha_{ADAR1}$  were determined by curve fitting  $k_{ex}$  of the imino protons as a function of  $f_Z$  with Eq. 2 (Fig. 2).<sup>10</sup>

In order to estimate the reliability of the proposed model in the previous study, we performed the iterative non-linear curve fitting  $k_{ex}$  of the imino protons in the CA6- $Z\alpha_{ADAR1}$  and TA6- $Z\alpha_{ADAR1}$  complexes as a function of  $f_Z$  with Eq. 2 using program Origin 7. The upper and lower confidence limits on the  $k_{ex}$  data of CA6 and TA6 complexed with  $Z\alpha_{ADAR1}$  were evaluated by iterative non-linear curve fitting and the 95% confidence bands of the  $k_{ex}$  data are shown in Fig. 2. This result shows that the *active-mono* B-Z transition mechanism, which was proposed in the previous study,<sup>10</sup> is suitable approach to understand the DNA sequence discrimination step of the  $Z\alpha_{ADAR1}$  protein during B-Z transition.

The relative population of each complex state (such as **B**, **BP**, **ZP**, and  $\mathbf{ZP}_2$ ) as a function of the P/N ratio was determined from the  $f_Z$  and  $k_{ex}$  data, which were reported in previous study,<sup>10</sup> as the following procedure. First, the **[BP]** values are calculated from the exchange data,  $k_{ex}$ ,  $k_{ex}^B$ , and  $k_{ex}^{BP}$ , by using Eq. 3:

$$[\mathbf{BP}] = \frac{k_{ex} - k_{ex}^B}{k_{ex}^{BP} - k_{ex}^B} (1 - Z_t) \quad (3)$$

where  $Z_t$  are determined from relative peak intensities of the imino proton resonances of the Z-form DNA. Second, the **[B]** values can be calculated by using the equation,  $[\mathbf{B}] = 1 - Z_t - [\mathbf{BP}]$ . Third, the concentration of the  $\mathbf{ZP}$  state (**[ZP]**) is calculated from the flowing relation,  $[\mathbf{ZP}] = [\mathbf{BP}]/K_{BZ}^1$ . Forth, the concentration of the  $\mathbf{ZP}_2$  state (**[ZP<sub>2</sub>]**) can be calculated by using the equation,  $[\mathbf{ZP}_2] = Z_t - [\mathbf{ZP}]$ . The relative populations (including estimated errors) of the **B**, **BP**, **ZP**, and  $\mathbf{ZP}_2$  states in the CA6- $Z\alpha_{ADAR1}$  and TA6- $Z\alpha_{ADAR1}$  complexes as a function of the P/N ratio are shown in Fig. 3 and 4, respectively. Finally, the concentration of free  $Z\alpha_{ADAR1}$  (**[P]**) could be calculated by the Eq. 4:

$$[\mathbf{P}] = P_t - [\mathbf{BP}] - [\mathbf{ZP}] - 2[\mathbf{ZP}_2] \quad (4)$$

where  $P_t$  is the total concentration of  $Z\alpha_{ADAR1}$ .

From these concentrations, the association constants,  $K_a^{BP} =$

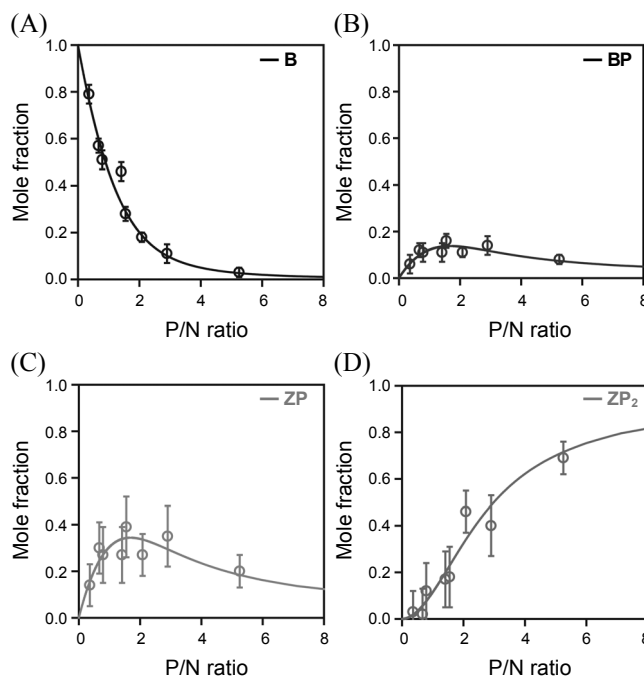


**Figure 3.** The relative populations of the (A) **B**, (B) **BP**, (C) **ZP**, and (D)  $\mathbf{ZP}_2$  states within total DNA populations of the CA6 complexed with  $hZ\alpha_{ADAR1}$  determined at 25°C. Solid lines are simulated relative population of each complex state determined as described in text.

$[\mathbf{BP}]/[\mathbf{B}][\mathbf{P}]$  and  $K_a^{ZP_2} = [\mathbf{ZP}_2]/[\mathbf{ZP}][\mathbf{P}]$ , for the CA6- $Z\alpha_{ADAR1}$  and TA6- $Z\alpha_{ADAR1}$  complexes were calculated. The  $K_a^{BP}$  and  $K_a^{ZP_2}$  values of CA6- $Z\alpha_{ADAR1}$  complex are  $3.9 \pm 1.3 \times 10^3$  and  $5.5 \pm 1.9 \times 10^3$ , respectively.<sup>10</sup> This means that, unlike the  $d(\text{CGCGCG})_2$ - $Z\alpha_{ADAR1}$  complex,<sup>9</sup> the  $Z\alpha_{ADAR1}$  protein can bind to the **B** and  $\mathbf{ZP}$  complex states with similar binding affinity. The relative population of each complex state for the CA6- $Z\alpha_{ADAR1}$  complex as a function of the P/N ratio could be calculated from these association constants and equilibrium constants for B-Z transition and the results are shown in Fig. 3 (solid lines). It was observed that **[B]** was gradually decreased, but **[BP]** and **[ZP]** were increased as the P/N ratio increased up to 2 (Fig. 3). In addition, the observation that **[BP]** is always smaller than **[ZP]** could be explained by the fact that  $K_{BZ}^1 < 1$  (Fig. 3). When the P/N ratio rose to 2, the  $\mathbf{ZP}_2$  complex was dominantly produced but **[BP]** and **[ZP]** were decreased as the P/N ratio increased because the added **P** preferentially bound to the  $\mathbf{ZP}$  complex rather than the **B** and **BP** (Fig. 3).

Similarly, the  $K_a^{BP}$  and  $K_a^{ZP_2}$  values of the TA6- $Z\alpha_{ADAR1}$  complex are  $2.5 \pm 0.9 \times 10^3$  and  $3.5 \pm 1.3 \times 10^4$ , respectively.<sup>10</sup> The relative population of each complex state for the TA6- $Z\alpha_{ADAR1}$  complex as a function of the P/N ratio are shown in Fig. 4 (solid lines). Similar to the CA6- $Z\alpha_{ADAR1}$  complex In the both complexes, it was observed that **[B]** was gradually decreased, but **[BP]** and **[ZP]** were increased as the P/N ratio increased up to 2 (Fig. 4). However, contrast to the CA6- $Z\alpha_{ADAR1}$  complex, it was observed that **[BP]** is always larger than **[ZP]**, indicating that  $K_{BZ}^1 > 1$ , (Fig. 4). When the P/N ratio rose to 2, the  $\mathbf{ZP}_2$  complex was dominantly produced but **[BP]** and **[ZP]** were decreased as the P/N ratio increased like CA6 (Fig. 4).

Interestingly, the simulated population (solid line in Fig. 3 and

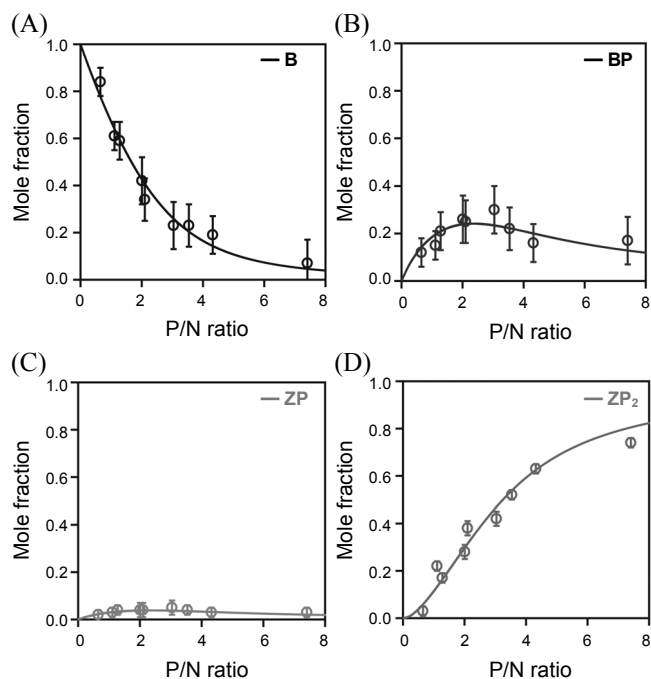


**Figure 4.** The relative populations of the (A) B, (B) BP, (C) ZP, and (D) ZP<sub>2</sub> states within total DNA populations of the TA6 complexed with hZ<sub>ADAR1</sub> determined at 15°C. Solid lines are simulated relative population of each complex state determined as described in text.

4) of each complex data determined from the association constants and equilibrium constants for B-Z transition well matched to the experimental value (symbol in Fig. 3 and 4) determined from the  $f_Z$  and  $k_{ex}$  data. This indicates that our approach is able to calculate successfully the concentrations of the intermediate state during B-Z transition. This correlation between the relative population of each complex state and the P/N ratio as shown

Fig. 3 and 4 can explain how the Z<sub>ADAR1</sub> protein recognizes the d(CGCGCG) sequence from d(CACGTG) and d(CGTACG) sequences in a long genomic DNA.

In summary, we derived the relative population of each complex state, which is thought to be produced during B-Z transition induced by Z<sub>ADAR1</sub>, as a function of the P/N ratio. This approach provides the insight into the active B-Z transition mechanism and DNA sequence discrimination step of human Z-DNA binding protein, ADAR1.

**Acknowledgments.** This Work was supported by the National Research Foundation of Korea Grants [2010-0014199; NRF-C1ABA001-2010-0020480 to J.-H.L.] funded by the Korean Government (MEST).

### References

1. Rich, A.; Nordheim, A.; Wang, A. H. *Annu. Rev. Biochem.* **1984**, *53*, 791.
2. Herbert, A.; Rich, A. *J. Biol. Chem.* **1996**, *271*, 11595.
3. Herbert, A.; Rich, A. *Genetica* **1999**, *106*, 37.
4. Herbert, A. G.; Rich, A. *Nucleic Acids Res.* **1993**, *21*, 2669.
5. Herbert, A.; Alfken, J.; Kim, Y. G.; Mian, I. S.; Nishikura, K.; Rich, A. *Proc. Natl. Acad. Sci. USA* **1997**, *94*, 8421.
6. Herbert, A.; Schade, M.; Lowenhaupt, K.; Alfken, J.; Schwartz, T.; Shlyakhtenko, L. S.; Lyubchenko, Y. L.; Rich, A. *Nucleic Acids Res.* **1998**, *26*, 3486.
7. Schwartz, T.; Rould, M. A.; Lowenhaupt, K.; Herbert, A.; Rich, A. *Science* **1999**, *284*, 1841.
8. Ha, S. C.; Choi, J.; Hwang, H. Y.; Rich, A.; Kim, Y. G.; Kim, K. *Nucleic Acids Res.* **2009**, *37*, 629.
9. Kang, Y.-M.; Bang, J.; Lee, E.-H.; Ahn, H.-C.; Seo, Y.-J.; Kim, K. K.; Kim, Y.-G.; Choi, B.-S.; Lee, J.-H. *J. Am. Chem. Soc.* **2009**, *131*, 11485.
10. Seo, Y.-J.; Ahn, H.-C.; Lee, E.-H.; Bang, J.; Kang, Y.-M.; Kim, H.-E.; Lee, Y.-M.; Kim, K.; Choi, B.-S.; Lee, J.-H. *FEBS Lett.* **2010**, *584*, 4344.